Bull. Inst. Chem. Res., Kyoto Univ., Vol. 72, No. 2, 1994

REVIEW

Information about Interaction of Implanted Ions with Amorphous Silica obtained from Structural Defects

Hideo HOSONO*, Hiroshi KAWAZOE*
and Yoshihiro ABE**

Received April 1, 1994

Effects of implantation of non-noble gas ions into amorphous silica were deduced from an analysis of structural defects produced during implantation. The predominant defect produced by implantation is a Si-Si homobond similar to that in an Si_2H_6 molecule. The ratio of concentrations of the homobond to the implanted ion is proposed as a measure of the strength of chemical interaction of implanted ions with the substrate. An analysis of equilibrium between two types of oxygen deficient defects and the FT-IR ATR spectra of network vibrations lead to a conclusion that the implanted silica layers have high fictive temperature which cannot be attained by conventional techniques.

KEY WORDS: Ion Implantation/ Amorphous Silica/ Structure Defects/ Si-Si homobond/ Fictive Temperature/ FT-IR ATR Spectra/ ESR/ E' Center

1. INTRODUCTION

Ion implantation is a technique which can significantly modify the surface and near-surface region of materials and has been applied mainly to semiconductors and metals. Recently, attention has been directed to application of this technique to fabrication of optical integrated circuits on a planar glass.[1-3] Ion implantation may provide precise control of ion concentrations and profiles. Silica glass has several advantages over other glasses as an amorphous substrate material with respect to basic research and applications. It has a simple stoichiometry and can be prepared with low (<10 ppb) concentrations of cation. Significant knowledge about structural defects has accumulated over the last three decades.[4-6] Furthermore, the refractive index of silica glass is low (1.46) and increases by implantation of all the ion species reported.[2,7] These features are favorable for fabrication of integrated optical waveguides on amorphous silica.

The properties of implanted layers are determined by the amount and state of implanted ions and intrinsic defects produced during implantation. Therefore, understanding relations between the defects and implanted ions is important. Characterization of structural defects will give a novel clue to this problem. In particular, we anticipate that information about the formation of oxygen-deficient type structural defects may provide information on the chemical

* 細野秀雄，川副博司：Research Laboratory of Engineering Materials, Tokyo Institute of Technology, Nagatsuta, Midori-ku, Yokohama, 227, Japan.
** 阿部良弘：Department of Materials Science and Engineering, Nagoya Institute of Technology, Gokiso-cho, Showa-ku, Nagoya 466, Japan.

interaction of implanted ions with substrate structure, e.g. with oxygen to form oxides. One consequence of such an interaction would be a high concentration of oxygen-deficient type structural defects in the implanted layers. An extremely high fictive temperature is expected in the thin layers due to dissipation of the kinetic energy of implanted ions.[3]

In this paper we review our data on structural defects in silica glass produced during implantation and interaction of implanted ions with silica glass substrate obtained through measurement of concentrations and types of point defects. Emphases are placed on chemical interaction of implanted ions with oxygens in silica network and estimation of fictive temperature of implanted layers.

2. EXPERIMENTAL OUTLINE

Type III silica glass was chosen because some type IV silica glasses give an intense absorption band in the vacuum uv (vuv) region in the as-delivered state.[8] Glass plates, 1.0 mm or 0.5 mm thick, were used as substrate. Elements of the first transition series, silicon or nitrogen +1 ions were implanted into substrates at room temperature to doses (nominal) ranging from 0.3×10^{16} to 6×10^{16} cm^{-2}. The acceleration voltage and dose rate were 160 keV and 2.5 $\mu A/cm^2$, respectively. Implantation depth profiles were determined by Rutherford backscattering (RBS) technique.

Vacuum uv and conventional uv absorption spectra were measured over the wavelength of 900~150 nm. Photoluminescence was measured in the uv region. Unless otherwise noted, these measurements were carried out at room temperature. EPR spectra were measured with an *X*-band spectrometer at 300, 110, 77 or 4.2 K. Total attenuated reflection spectra (ATR) were measured using a Fourier Transform infrared spectrometer with an MCT detector cooled with liquid N_2. Germanium (refractive index 4.0) was used as an internal reflection element for the ATR measurement.

3. RESULTS

3.1 Vuv-uv absorption

Figure 1 shows typical examples (Cr-implanted) of vuv and uv absorption spectra of the implanted samples.[9] Absorption coefficient in the region of the tail ($\approx$7.5 eV) of the absorption edge for the unimplanted substrate was <0.01 cm^{-1}. An intense and a weak but distinct absorption peaks are resolved around 7.5 and 5 eV, respectively. Intensities of both bands increased with dose. Similar results were obtained for the substrates implanted with other ions expect N and Cu ions. The intensities of the 7.5 eV and 5 eV bands in the N-implanted samples were approximately 1/10 those in the samples implanted with the other ions. No information about these two bands were obtained for samples implanted with Cu ions to a dose of $>3\times10^{16}$ ions/cm^2 because intense absorptions due to Cu ions became predominant.

3.2 EPR spectra

No EPR signals were detected for the substrate before implantation under operation conditions described below. Figure 2 shows EPR spectra of the substrate after Cr-implantation.[9] Three types of signals are noted except a signal centered at $g=1.97$, which is not due to intrinsic defects but to paramagnetic states of implanted Cr ions. A signal having a

characteristic shoulder at $g=2.067$ is assigned to a peroxy radical (POR)[10] on the basis of the g-values. No nonbridging oxygen hole centers (NBOHC) are resolved. Based on the close

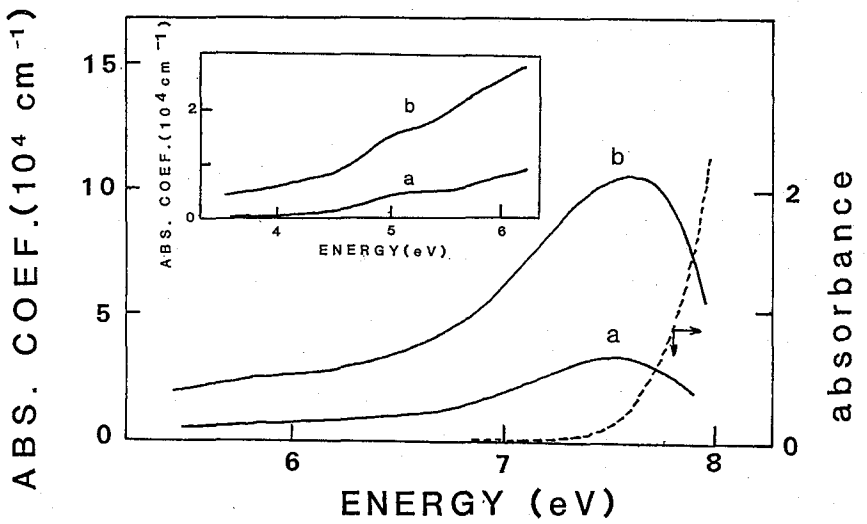

Fig. 1. Vacuum uv and uv absorptions induced by ion implantation. (a) Cr 0.5×10^{16} ions/cm^2, (b) Cr 3×10^{16} ions/cm^2. The dashed trace is the absorption spectrum of unimplanted substrate. The thickness of implanted layers are assumed to be 140 nm.

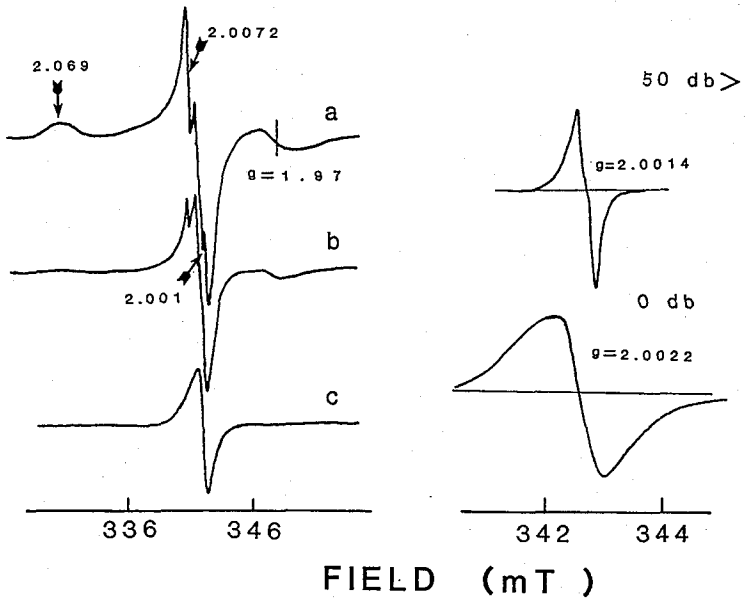

Fig. 2. EPR spectra of Cr-implanted substrates. Changes with dose (left). a, 0.5×10^{16}; b, 3×10^{16}; c, 6×10^{16} ions/cm^2. Small arrows indicate POR. The component due to "X" signal is indicated by big arrows. Changes with microwave power (right). Sample; Cr 6×10^{16} ions/cm^2. The spectrometer sensitivity for measuring the top signal is 30 times greater than that for the bottom signal.

similarity of g-values, of line shape in neutron-bombarded silica glass,[11] and of microwave saturation behavior (easily saturable compared with other signals, but less saturable than standard E' center), one component is assigned to an E' center.[12]

In addition to the POR and E' center components, an absorption with a slightly asymmetric shape is dominant in the spectrum of samples implanted to a dose of 6×10^{16} ions/cm^2 measured at a power level of 200 mW (110 K). This signal, called "X" temporarily, can be easily resolved from E'-center components produced by implantation. The "X" signal has a line shape that is almost isotropic, a g-value equal to 2.0022, linewidth of 0.8 mT, and does not saturate appreciably up to the 200 mW level at 110 K. Saturation behavior of a standard E' center, E'

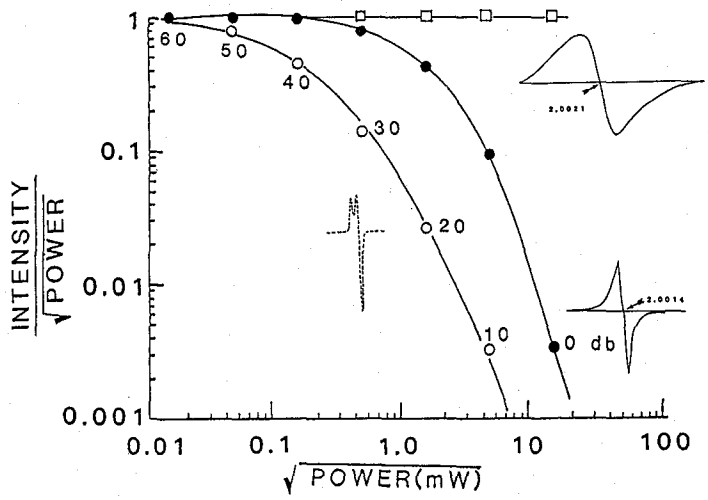

Fig. 3. Comparison of Microwave power saturation behavier among standard E' center (○), E' center (●)produced by implantation, and E' type center (□) associated with Si-Si bond.

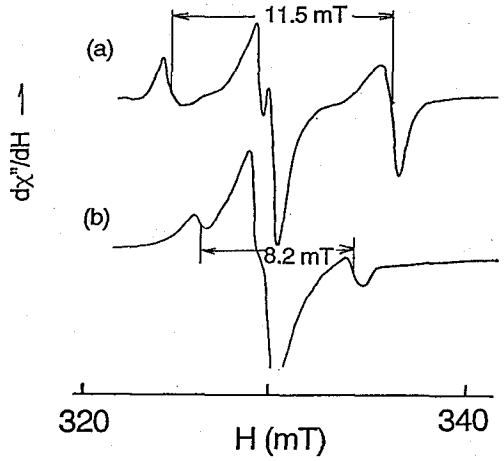

Fig. 4. EPR spectra of the substrates implanted with (a) ^{14}N and (b) ^{15}N ions to a dose of 3×10^{16} ions/cm^2. The spectra were obtained at 77 K and 200 mW.

center produced by implantation and the "X" signal is summarized in Fig. 3. These paramagnetic centers are observed commonly in the substrate implanted with other transition metal ions except copper and nitrogen. The "X" center was not observed in Cu- or ^{14}N-implanted substrtaes.

The EPR spectra of N-implanted substrates differ.[14] The separation between the lowest field component and the highest field component is 11.5 mT. Figure 4 shows the EPR spectrum of the substrate implanted with $^{14}N^+$ or $^{15}N^+$. In the ^{15}N-implanted sample, the signal with a separation of 11.5 mT appearing in the ^{14}N-implanted sample is missing, and components with a separation of 8.2 mT appear.

3.3 Fourior-transform infrared attenuated reflection spectra

Fourior-Transform Infrared Attenuated Total Reflection (FT-IR ATR) spectra[15] was an appropriate method to measure the IR spectra of implanted layers because penetration depth of infrared radiation is 0.2～1.0 μm[16] depending on the wavelength. Figure 5 shows FT-IR ATR spectra of silica glasses before and after implantation.[16] Since no significant line shape difference was seen among the Si-, P-, and N-implanted substrates, it is evident that no bands relevant to the implanted ions appear and the spectral changes observed are due to modification in the substrate structures by implantation. Three bands centered around 1,100, 1,000 and 800 cm^{-1} were resolved, and are assigned to w_4 (LO), w_4 (TO) and w_3, respectively.[17] Comparing the band positions in the spectrum of the implanted face with those of the unimplanted face, it is obvious that w_4 (LO) and w_4 (TO) shift to a lower frequency side whereas w_3 shifts in the opposite direction.

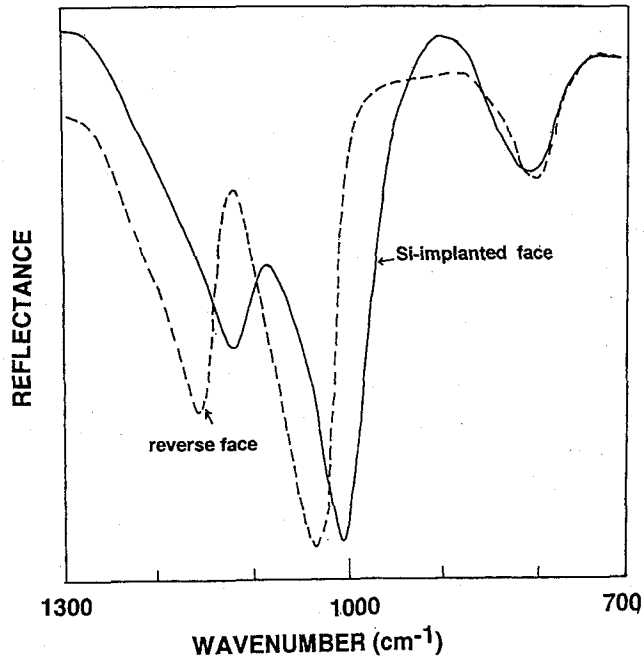

Fig. 5. FT-IR ATR spectra. ——, Si 6×10^{16} ions/cm^2 implanted; – – –; unimplanted face.

4. DISCUSSION

4.1 Defect responsible for the 7.5 eV band

Two structural models have been proposed for this band; one is the POR,[10] which is paramagnetic and is due to an oxygen-excess-type defect. Another is the Si-Si homobond,[18,19] which is diamagnetic and an oxygen-deficient type defect. Since the POR concentrations decrease with dose, POR cannot be a major part of the 7.5 eV band. The contribution of POR to the band, which can be estimated from the EPR data and absorption cross-section (1.3×10^{-16}cm^2) of POR, is less than 7 %. Here, let us suppose as a first approximation that the absorptivity at the apparent peak of the band is controlled completely by Si-Si homobonds. Then, the homobond concentration can be evaluated by using the reported cross section(8×10^{-17} cm^2)[18] of the homobond, which is close to that (6×10^{-17} cm^2)[20] of the corresponding band (7.56 eV) of Si_2H_6 molecule.

4.2 Structural origin of the 5 eV band

Four structural models have been proposed so far, to our knowledge for the 5 eV band. Tohmon *et al.*[21] assigned the 7.5 eV band and 5.0 eV band to singlet-to-singlet and a singlet-to-triplet transitions of Si-Si bond electrons, respectively. Skuja *et al.*[22] proposed a two-coordinated silicon (-Si-). In this model the 5 eV band is due to the singlet-to-singlet transition of the 3S lone pair electrons on the Si atom. Thus, the absorption should be unbleachable by uv-irradiation.

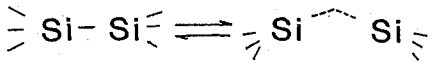

Fig. 6. Defect configurations for the two types of oxygen-deficient centers.

Imai *et al.*[18] proposed two types of oxygen-deficient defects as shown in Fig. 6, a Si-Si homobond and a neutral oxygen vacancy with transitions of 7.5 eV and 5 eV, respectively. They found[18,23] that the 5 eV band is bleachable by irradiation with KrF (5 eV) or ArF (6.4 eV) excimer laser light[23] without accompanying changes in the intensity of the 7.5 eV band and that

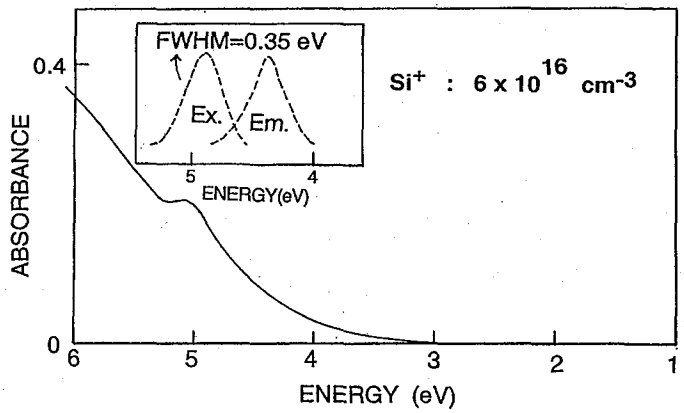

Fig. 7. Uv absorption spectrum of the substrate implanted with Si ion to dose of 6×10^{16} ions/cm^2. The inset are emission and excitation spectra.

photo-excitation of the 5 eV band gives an emission band with FWHM of 0.35 eV centered at 4.3 eV. Recently, Hosono and Weeks,[24] have found in -irradiated silica glasses that POR and the 5 eV band with 0.8 eV in FWHM are bleached out by illumination with 5 eV light, suggesting that POR gives 5 eV optical band (there is a 5 eV transition of the O_2^- molecular ions in alkali halides, J. Rolfe, F.R. Lipsett, and W.J. King, Phys. Rev. 123, 447~453 (1961)).

As shown in Fig. 7, an emission band with $\approx$0.3 eV width is observed by photoexcitation of the 5 eV band around 4.3 eV even in the sample for which POR signal is not seen. These ovservations agree with the characteristics of the neutral oxygen vacancy model. Therefore, we conclude that the 5 eV band appearing in ion-implanted silica is due mainly to the neutral oxygen vacancy.[23] The concentrations of the oxygen vacancy can be evaluated from the absorptivity and cross-section (2×10^{-17} cm^2).[18]

4.3 Paramagnetic defects

4.3.1 Defect structure of "*X*"-center

No EPR signal similar to the *X*-signal has been reported in a-SiO_2 irradiated by ionizing photons, to our knowlidge. A report examining paramagnetic defects in nonstoichiometric amorphous SiO_x provides a basis for proposing a model for the "*X*" center. Holzankampfer et al.[23] measured EPR spectra in as-deposited and He^+-bombarded a-SiO_x films over a wide range of x ($0\lesssim x\lesssim 2$), reporting the variation in the g-values and linewidths of E'-type centers as a function of x. Both of g-value (2.0022) and linewidth (0.8 mT) of the "*X*" signal are close to those of E'-type signal in $x=1.5$. The less-saturable nature of the para-magnetic states in these oxygen-degicient materials is consistent with that of the "*X*" center. Based on the model proposed for the center in a-$SiO_{1.5}$, the "*X*" -center has s structure (Fig. 8) which is obtained by replacing one of the three oxygens in a prototypical E'-center by a Si atom, i.e. we assign the "*X*" -signal to an E'-type defect associated with a Si-Si homobond.

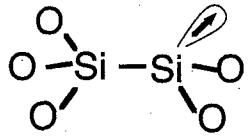

Fig. 8. A model of defect (E' type center) responsible for the "*X*" signal.

4.3.1 N-associated center

On the assumption that the separation (11.5 mT) in the N-implanted sample and the separation (8.2 mT) in the ^{15}N-implanted sample are due to a ^{14}N nucleus (nuclear spin 1) and a ^{15}N nucleus (1/2), respectively, the ratio (0.70) of the isotropic hf separation agrees well that (0.71) of magnetogyric ratio of ^{14}N to ^{15}N. Therefore we conclude that the signal with a separation of 11.5 mT is the hf absorption due to a ^{14}N nucleus. Three N-associated centers have been reported in glasses so far,[27] a hole-trapped nitrogen bridging two silicons, Si-N-Si, an electron-trapped nitrogen anion substituting an SiO_4^{4-} vacancy, and a NO_2 molecular having 17 electrons. These three centers can be discriminated easily by the magnitude of the ^{14}N hf coupling constant. An approximate magnitude of isotropic hf separation due to a ^{14}N is 3.6 mT for Si-N-Si, 1.9 mT for an electron-trapped nitrogen anion at the site of an SiO_4^{4-} vacancy, or 5.6 mT for a NO_2 molecule. We assign a paramagnetic species giving this hf absorptions as a NO_2 molecule referring to the magnitude of hf separations of these N-related centers. Figure 9 shows

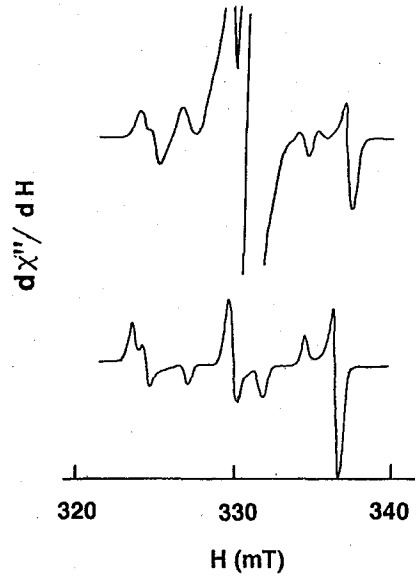

Fig. 9. EPR spectra of N-implanted substrate. (Top) measured at 4.2 K. Note that outer field components are resolved compared with the line shape at 77 K (trace a in Fig. 7). Microwave power; 1 uW. A doublet with an aaproximately 7.0 mT separation is not due to NO_2 molecules but is due to E' center variant containing an Si-H bond. (Bottom) powder pattern calculated using the following EPR parameters; $g_1=1.9914$, $g_2=2.0023$, $g_3=2.0059$, $A_1=4.7$ mT, $A_2=6.6$ mT, $A_3=5.0$ mT.

the EPR spectra of the ^{14}N-implanted substrate measured at 4.2 K together with a powder pattern of an NO_2 molecule calculated using EPR parameters reported for NO_2 immobilized in solids.[28] Decreasing temperature to 4.2 K does not change the magnitude of the separation (11.5 mT) between the outer components but improves the resolution of the outer field components. These results suggest that the NO_2 molecules are immobilized in the silica network and broadening observed is attributed to thermally activated librational motions of the molecules.[28] The concentration of NO_2 molecules is to an approximate 1% of concentrations of implanted N ions.

4.4 Interaction of implanted ions with substrate structure

Although NBOHC formed via radiolysis of Si-OH is the dominant oxygen-related paramagnetic center in 'wet' silica irradiated with ionizing-photons,[4] only the POR is observed in the implanted substrate. We suggested that this result indicates that displacement effects play an essential role in the formation of defects in implanted silica. Figure 10 shows the concentrations of diamagnetic and paramagnetic defects produced by implantation of chromium ions as a function of dose. It is obvious from the figure that the dominant defects produced are the Si-Si homo-bonds, and their concentrations are comparable with those of implanted ions at each dose level. Similar results are observed for implantation with other transition metal ions as shown in Fig. 11.

The equivalence of the homobond and implanted cation concentrations is attributed,

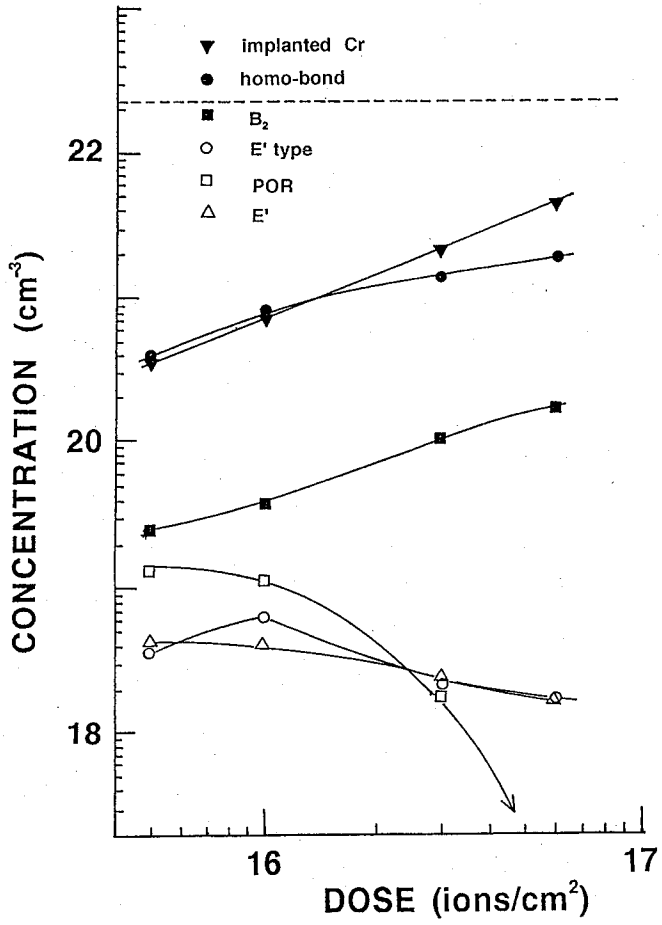

Fig. 10. Dose dependence of concentrations of intrinsic structural defects produced by implanatation. The dashed line indicates the concentration of Si atoms in the substrate.

tentatively, to chemical interactions of implanted ions with substrate ions. The implanted ions, therefore, attract oxygens as ligands so as to reserve local electroneutrality. If the chemical interaction of an implanted ion with oxygen is strong, the implanted ions reacts with some of the oxygens displaced from the glass network to form oxides, leaving Si-Si homobonds and neutral oxygen vacancies. According to this analysis, the concentrations of these defects will be determined by the number and mean valence of implanted ions participating in oxide formation.

Here, we will consider the state of implanted ions by applying these indicators. Since homobond concentrations are similar for the same dose of the transition series of ions, a fraction of the implanted transition metal ions are assumed to form oxides. The significant decrease in the ratio of homobondd to implanted ions observed for doses of $>3\times10^{16}$ ions/cm^2 indicates a reduction in oxide formation. This reduction may be a consequence of forming of metallic particles or colloids. Since atoms in metallic colloids do not react chemically with oxygens in the substrate, they do not contribute to the formation of the homobonds. An extreme case is found in Cu-implanted samples. Copper-implanted samples give no E'-type center but POR and E'-

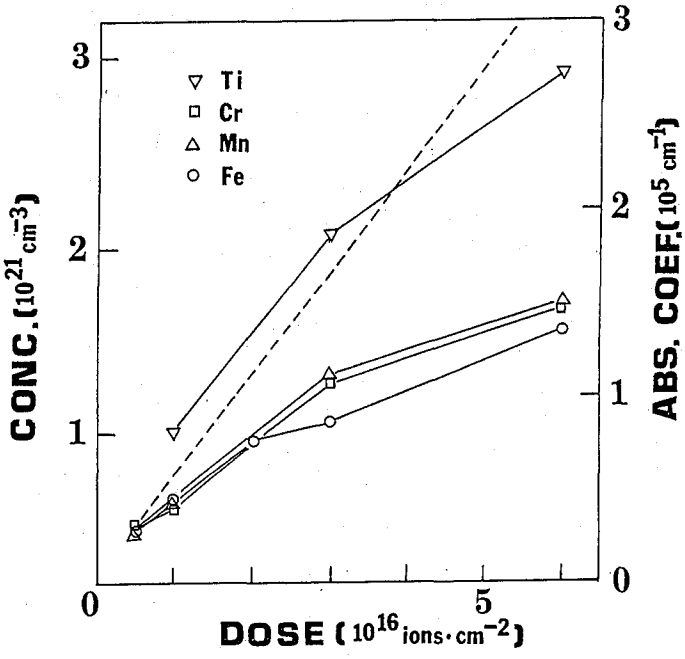

Fig. 11. Dose dependence of Si-Si homobond concentrations. The broken line denotes implanted ion concentrations evaluated from the RBS spectra.

centers.[13] These results are the same as those in neutron-bombarded silica.

4.5 *Fictive temperature*

Since energetic incoming ions dissipate their energies in a very short time in substrates, it is expected that implanted layers have a structure corresonding to high temperatures. Here, we will make an estimation of the T_f of the implanted layers by two different ways, i.e. the first way is to use information about two types of oxygen-deficient defects produced by implantation, and another way is based on information about network vibrations.

First, we will estimate the T_f by the first way. A thermal equilibrium is assumed between the configurations of the Si-Si homobond and neutral oxygen vacancy as Fig. 6. The homobond configuration is more stable than the vacancy configuration.[29] The enthalpy difference between these configurations is 1 eV, which was evaluated experimentally by using silica glass prepared by the CVD-soot remelting process.[18] The equilibrium constant K evaluated from Fig. 10 is 10^{-1} over the dose range examined, which is about 3 orders of magnitude greater than that (5×10^{-4}) in silica glass with T_f=1,300~1,600 K. Provided that this enthalpy difference remains unchanged, the T_f in the implanted layers is estimated to be 4,000 K.

Second, we will make an estimation of the T_f byanalyzing the FT-IR ATR spectra of the implanted sample. The opposite directions of the w_3- and w_4-shifts upon implantation indicate that the shifts observed are not attributed to the formation of non-bridging oxygens by implantation because w_3- and w_4-shift to a lower frequency upon introduction of network modifying ions into SiO_2 glass.[30] The linear relationship between the w_i-shift and T_f of silica glass was reported by Galeener in ref. 17. According to this report, w_4-shifts to a low wavelength

side and w_3 moves to a higher wavelength side with increasing T_f. The magnitude ($-32\ cm^{-1}$ for w_4 (LO) and $-24\ cm^{-1}$ for w_4 (TO)) of the shift observed has been not attained in quenching experiments of bulk SiO_2 glass, to our knowledge. The shift of w_4 (w_3) is only -12 (-5) cm^{-1} when the T_f is changed from 900 to 1,550 °C.[17] Provided that the slopes in the w_i vs. T_f remain unchanged, the T_f is estimated to be 3,000~4,000 K, which is similar to the T_f evaluated by the first way. It is interesting that the two ways based on quite different basis give the similar T_f, 3,000~4,000 K. These values are close to the T_f, which was estimated from T_f-dependent Raman bands, in neutron-bombarded SiO_2 glass.[17] We suppose that realization of a state corresponding to extremely high temperatures is associated closely with the "thermal spike" model of particle irradiation damage. Local heating due to energy generated in the collision of energetic ions with the substrate melts a microscopic volume around the sites of the primary knocked-on atoms and these extremely small volumes are rapidly quenched. Realization of such a high fictive temperature, which cannot be realized by conventional techniques, may explain some results characteristic of ion-implanted silica such as the change in chemical durability, an extremely high ratio of a low valence state to a high valence state for multi-valence ions,[31] and an anion distribution proper to an ion-beam-induced amorphous state.[32] Detailed discussion was made on ref. 16.

5. SUMMARY

We reviewed our data on structural defects produced by implantation and on interaction of implanted ions with amorphous SiO_2 substrate. The conclusions obtained are that:

(1) Si-S homobond are formed, and their concentrations are comparable with those of implanted ions with the exception of Cu.

(2) The ratio of the Si-Si homobond to implanted ions is a measure of the strength of chemical interaction of the implanted ion with the oxygen in the substrate structu

(3) Peroxy radical is produced as a dominant oxygen-related paramagnetic defect. No nonbridging oxygen hole center is seen even in 'wet' silica substrate. These results show that displacement process plays an essential role in the formation of defects in implanted silica.

(4) The implanted layers have high fictive temperatures, which can not be attained by conventional techniques.

6. ACKNOWLEDGMENTS

The author would like to thank Professor H. Imagawa (Toyo Univ., Japan) for vuv measurements, Dr. R.A. Zuhr (Oak Ridge National Lab., USA) for RBS measurements, and Professor Robert A. Weeks (Vanderbilt University) for helpful discussion.

REFERENCES

(1) P. Mazzoldi and G.W. Arnold, chap. 5, in Ion Beam Modification of Insulators, edited by P. Mazzoldi and G.W. Arnold, Elsevier, Amsterdam (1987).
(2) P.D. Townsend, "An Overview of Ion-Implanted Optical Waveguide Profiles", *Nucl. Instr. Methods. Phys. Res.*, **B46**, 18–25 (1990).
(3) G.W. Arnold, "Ion Implantation Effects in Glasses", *Rad. Eff.*, **65**, 257–70 (1982).
(4) D.L. Griscom, "Defects in Glass", *J. Non-Crtst. Sol.*, **73**, 51–77 (1985).
(5) F.L. Galeener, D.L. Griscom and F.L. Galeener (edited), Defects in Glasses (Mat. Res. Soc. Sym. Pros.

Vol. 61), (1986).
(6) R.A. Devine, The Physics and Technology of Amorphous Silica, Plenum (1988).
(7) A.P. Webb and P.D. Townsend, "Refractive Index Profiles Induced by Ion Implantation into Silica", *J. Phys. D: Appl. Phys.*, **9**, 1343–54 (1976).
(8) I.P. Kaminow, B.G. Bagley and C.G. Olson, *Appl. Phys. Lett.*, **32**, 98–99 (1978).
(9) H. Hosono and R.A. Weeks, "Structural Defects in Chromium-Ion-Implanted Vitreous Silica", *Phys. Rev.*, **B40**, 10543–49 (1989).
(10) M. Stapelbroak, D.L. Griscom, E.J. Friebele and G.H. Sigel, Jr., "Oxygen-Associated Trapped-Hole Centers in High-Purity Fused Silicas", *J. Non-Cryst. Sol.*, **32**, 313–326(1979).
(11) R.A. Weeks, in Interaction of Radiation with Solids", pp. 55–93, Edited by A. Bishay, Plenum, New York (1967).
(12) R.A. Weeks, "Paramagnetic Resonance of Lattice Defects in Irradiated Quartz", *J. Appl. Phys.*, **27**, 1376–81 (1956).
(13) H. Hosono, R.A. Weeks, H. Imagawa and R.A. Zuhr, "Formation of Oxygen-deficient Type Structual Defects and State of Ions in SiO_2 Glasses Implanted with Transition Metal Ions", *J. Non-Cryst. Sol.*, **120**, 250–255 (1990).
(14) H. Hosono, Y. Abe, K. Ohyoshi and S. Tanaka, "Effects of Co-implantation of Silicon and Nitrogen on Structural Defects and Si-N bond Formation in Silica Glass", *Phys. Rev. B*, **43**, 11966–970 (1991).
(15) G. Muller, K. Abraham and M. Schadach, "Quantitative ATR Spectroscopy: some basic considerations", *Appl. Optics*, **20**, 1182–90 (1981).
(16) H. Hosono, "Fourier Transform Infrared Attenuated Total Reflection Spectra of Ion-Implanted Silica Glass", *J. Appl. Phys.*, **69**, 8079–82 (1991).
(17) A.E. Geissberger and F.L. Galeener, "Raman Studies of Vitreous SiO_2 versus Fictive Temperature", *Phys. Rev.*, **B28**, 3266–71 (1983).
(18) H. Imai, K. Arai, H. Imagawa, H. Hosono and Y. Abe, "Two Types of Oxygen-deficient Centers in Synthetic Silica Glass", *Phys. Rev*, **B38**, 12772–75 (1988).
(19) H. Imai, K. Arai, H. Hosono, Y. Abe and H. Imagawa, "Dependence of Defects induced by Excimer Laser on Intrinsic Structural Defects in Synthetic Silica Glass", *Phys. Rev. B*, **44**, 4812–17 (1991).
(20) U. Itoh, Y. Toyoshima, H. Onoki, N. Washida and T. Ibuki, "Vacuum Ultraviolet Absorption Cross Sectionss of SiH_4, GeH_4, Si_2H_6, and Si_3H_8", *J. Chem. Phys.*, **85**, 4867–72 (1986).
(21) R. Tohmon, H. Mizuno, Y. Ohki, K. Sasagane, K. Nagasawa and Y. Hama, "Correlation of 5.0 eV amd 7.6 eV absorption bands in SiO_2 with Oxygen Vacancy", *Phys. Rev.*, **B39**, 1337–45 (1989).
(22) L.N. Skuja, A.N. Streletsky and A.B. Pakovich, "A New Intrinsic Defects in Amorphous SiO_2 : Twofold Coordinated Silicon", *Solid State Commun.*, **50**, 1069–72 (1984).
(23) K. Arai, H. Imai, H. Hosono, Y. Abe and H. Imagawa, "Two Photon Processes in Defects Formation by Excimer Lasers in Synthetic Silica Glass", *Appl. Phys. Lett.*, **53**, 1891–93 (1988).
(24) H. Hosono and R.A. Weeks, "Bleaching of Peroxy Radical in SiO_2 Glass with 5 eV Light", *J. Non-Cryst. Sol.*, **116**, 289–292 (1990).
(25) G.W. Arnold, "Ion-Implantation Effects in Noncrystalline SiO_2", *IEEE Trans. Nucl. Sci.*, **NS-20**, 220–3 (1973).
(26) E. Holzenkampfer, F.W. Richter, J. Stuke and V. Voget-Grote, *J. Non-Cryst. Sol.*, **32**, 327–338 (1979).
(27) D.L. Griscom, "Electron Spin Resonance", in Glass Science and Technology, Vol. 4B, chap. 3, Academic press (1990).
(28) E.J. Friebele, D.L. Griscom and T.W. Hickmott, "Nitrogen-Associated Paramagnertic Defect Centers in Sputtered SiO_2 Films", *J. Non-Cryst. Sol.*, **71**, 351–59 (1985).
(29) E.P. O'Reilly and J. Robertson, "Theory of Defects in Vitreous Silicon Dioxide", *Phys. Rev.*, **B27**, 3780–95 (1983).
(30) J.R. Ferraro and M.H. Manghnari, "Infrared Absorption Spectra of Sodium Silicate Glasses at High Pressure", *J.Appl. Phys.*, **43**, 4595–99 (1972).
(31) G. Whichard, H. Hosono, R.A. Weeks, R.A. Zuhr and R.H. Magruder, "Electron Paramagnetic Resonance Spectroscopy of Titanium-Ion-Implanted Sillica", *J. Appl. Phys.*, **67**, 1138–41 (1989).
(32) B.C. Sales, J.O. Ramey, L.A. Boatner and J.C. McCallum, "Structural Inequivalence of the Ion-Damage-Produced Amorphous State and the Glass State in Lead Pyrophosphate", *Phys. Rev. Lett.*, **62**, 1138–41 (1989).